JTTEE5 4:261-267

The Relationship Between the Microstructure and Thermal Diffusivity of Plasma-Sprayed Tungsten Coatings

S. Boire-Lavigne, C. Moreau, and R.G. Saint-Jacques

Tungsten and tungsten alloy coatings are candidate materials for plasma facing components of divertor plates in future fusion reactors. In normal operation, the sprayed coatings will be submitted to intense heat fluxes and particle bombardment. This work investigated the relationship between the microstructure of plasma-sprayed tungsten coatings and their thermal diffusivity as determined by the laser flash method. The microstructural investigation was carried out on copper-infiltrated coatings. Such a preparation technique permitted the measurement of the total true contact area between the lamellae within the tungsten coatings. The spraying atmosphere was found to strongly influence the interfacial contact between lamellae and coating thermal diffusivity.

1. Introduction

PLASMA-SPRAYED tungsten coatings are candidate materials for plasma facing components such as the divertor plates in the future International Thermonuclear Experimental Reactor (ITER) (Ref 1, 2). Because divertor plates are submitted to intense thermal loads, it is imperative to know their thermal response, which is related to their composition and microstructure. Plasma-sprayed coatings are formed by powders accelerated and heated in a plasma jet and sprayed onto a substrate. The particular microstructure of the sprayed coatings results from the accumulation of molten or partially molten droplets impinging on the already-solidified layers. The way the particles splat on the coating surface strongly influences the bonding between the lamellae and thus the thermal and mechanical properties of the coating.

The coating microstructure is commonly characterized by direct observation of the polished coating cross section under optical and scanning electron microscopes. However, standard metallographic preparation techniques may induce defects in the coating, making quantitative measurements difficult or even impossible (Ref 3, 4). As established by transmission electron microscopy, cohesion between lamellae is relatively low (Ref 5), which results in pullout during metallographic preparation (Ref 6). In order to limit such damage and avoid lamella delamination, the open porosity of the sprayed coatings was infiltrated with copper before metallographic preparation. Infiltration has two main advantages: copper acts as a glue, minimizing pullout, and it ensures good metallographic contrast between the lamella interfaces.

Keywords: microstructure, modeling, porosity characterization, thermal diffusivity, tungsten coating

S. Boire-Lavigne, INRS-Énergie et Matériaux, Varennes, Québec, Canada (presently at AMRA Technologies Inc., Montréal, Québec, Canada); **C. Moreau,** National Research Council of Canada, Industrial Materials Institute, 75 de Mortagne, Boucherville, Québec, J4B 6Y4, Canada; and **R.G. Saint-Jacques,** INRS-Énergie et Matériaux, Varennes, Québec, Canada.

Coatings were prepared according to an experimental plan based on the L8 $(2)^7$ Taguchi table used to optimize and highlight the influence of five spray factors on the coating thermal properties. Previous studies on the influence of the plasma spray factors (spraying atmosphere, arc gas, torch lateral speed, arc power, and powder feed rate) on the coating thermal diffusivity and microstructural parameters (lamella thickness, oxygen content, interlamellar contact, specific surface, and porosity) have already been published (Ref 6, 7). In these studies, it has been found that the spraying atmosphere has the most influence on the coating microstructure and thermal diffusivity.

This paper analyzes the influence of microstructural parameters on the thermal diffusivity of the sprayed coatings. One of the main challenges of this analysis was to characterize the quality of the interface between the tungsten lamellae. Image analysis was used to measure lamella thickness and interlamellar contact. The coating thermal diffusivity was computed using a model based on the observed microstructure elements of the coatings, and it was compared to experimental diffusivity values.

2. Thermal Diffusivity Model

Estimation of the thermal conductivity of the sprayed coatings is based on a model developed by McPherson (Ref 8). The model assumes that the microstructure of the coatings consists of a stacking of lamellae separated by imperfect interfaces (Fig. 1). These interfaces are composed of circular regions of true contact and no contact (interlamellar porosity). Conduction and convection heat transfers through interlamellar pores are neglected, because the size of the interlamellar porosity is near the mean free path of the gas molecule (Ref 8), and because at 300 K the thermal conductivity of gas in the interlamellar porosity is about 26×10^{-3} W/m·K and that of tungsten is about 140 W/m·K (Ref 2). At room temperature, radiation heat transfer is also assumed to be negligible.

Contrary to the model developed by McPherson for ceramic oxides (Ref 8), true contacts are not necessarily equivalent to the bulk material in metal coatings, because the presence of secon-

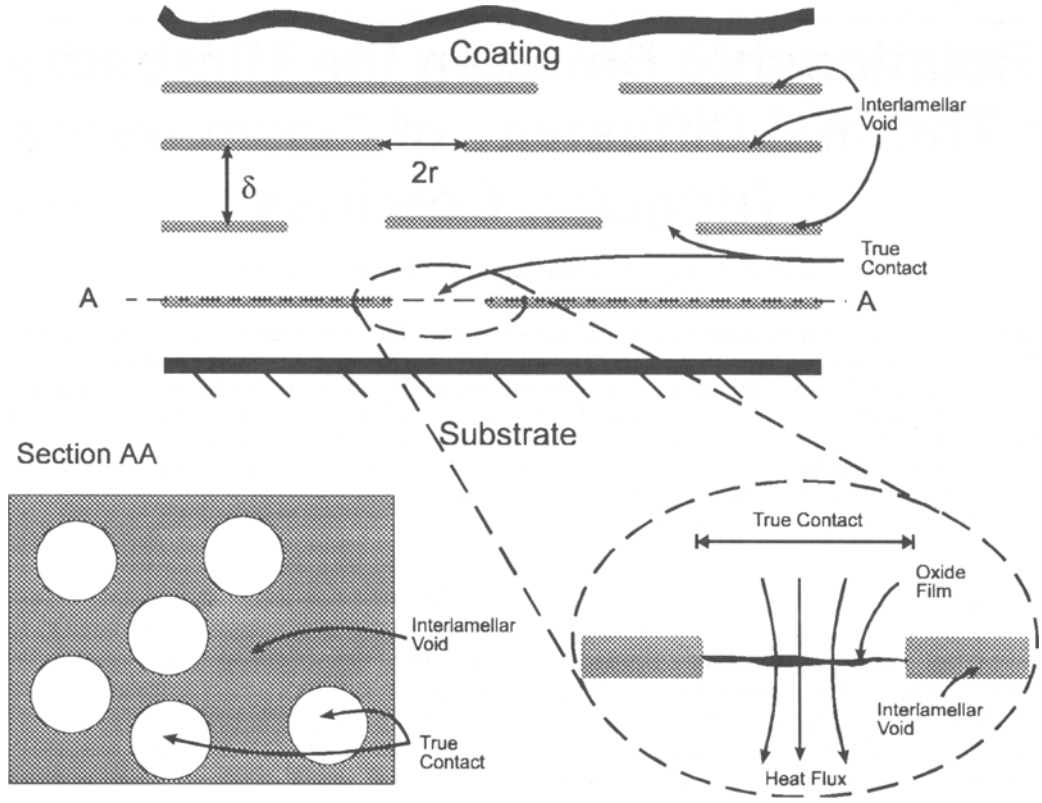

Fig. 1 Schematic view of the coating cross section microstructure

dary phases such as oxides could influence the thermal conductivity of the true contacts. The model considers the problem from the point of view of electrical resistance of metallic contacts (Ref 8). Using this analogy and the coating microstructure model illustrated in Fig. 1, the total thermal resistance R_T of the coating is the summation of the thermal resistances of the lamellae stacked in the through-thickness direction. The thermal resistance of a single lamella R_t is taken as the sum of the lamella material resistance R_L, the interfacial resistance of the true contacts R_i, and the oxide layer resistance in the true contact zones R_o:

$$R_t = N(R_L + R_i + R_o) = \frac{e}{\delta + \delta_o}(R_L + R_i + R_o) \qquad \text{(Eq 1)}$$

where N is the number of lamellae, δ is the lamella thickness, δ_o is the oxide layer thickness, and e is the coating thickness. The lamella material resistance is assumed to be related only to the lamella thickness and thermal conductivity. The interfacial resistance is directly obtained from the electric analog where the conductivity depends on the radius and number of true contact zones at the interface (Ref 8). The contribution of the oxide layer to the total resistance is assumed to be proportional to the thickness of the oxide layer and inversely proportional to the total surface of the true contact zones. Then the thermal resistances can be written as:

$$R_L = \frac{\delta}{\lambda_w} \quad R_i = \frac{1}{2nr\lambda_w} \text{ and } R_o = \frac{\delta_o}{\lambda_o \pi n r^2} \qquad \text{(Eq 2)}$$

where λ_w and λ_o are the thermal conductivities of tungsten and tungsten oxide, respectively; n is the number of true contact zones in parallel in a given interfacial plane; and r is the radius of these contact zones. When $\delta >> \delta_o$, the coating thermal conductivity λ_c is given by:

$$\frac{1}{\lambda_c} = \frac{R_T}{e} = \frac{(R_L + R_i + R_o)}{\delta} = \frac{1}{\lambda_w}\left(1 + \frac{1}{2nr\delta}\right) + \frac{\delta_o}{\lambda_o \pi n r^2 \delta} \qquad \text{(Eq 3)}$$

Thermal diffusivities for the tungsten α_W, oxide layer α_o, and coating α_c can be respectively written as:

$$\alpha_W = \frac{\lambda_W}{\rho_W C_{Pw}} \quad \alpha_o = \frac{\lambda_o}{\rho_o C_{Po}} \text{ and } \alpha_c = \frac{\lambda_c}{\rho_c C_{Pc}} \qquad \text{(Eq 4)}$$

where ρ_w, ρ_o, and ρ_c are the densities of tungsten, the oxide layer, and the coating, respectively, and C_{Pw}, C_{Po}, and C_{Pc} are the thermal capacities of tungsten, the oxide layer, and the coating, respectively.

The coating density ρ_c and the thermal capacity of the coating C_{Pc} are simply given by:

$$\rho_c = (1 - F - F_o)\rho_W + F\rho_{air} + F_o\rho_o \cong (1 - F)\rho_w \qquad \text{(Eq 5)}$$

$$C_{Pc} = (1 - F_o)C_{Pw} + F_o C_{Po} \cong C_{Pw} \qquad \text{(Eq 6)}$$

where F is the coating porosity; F_o is the oxide content, and ρ_{air} is the air density. The contribution of air and the oxide content are neglected because $\rho_W >> \rho_{air}$ and $F >> F_o$. Finally, the thermal diffusivity of the sprayed coating is:

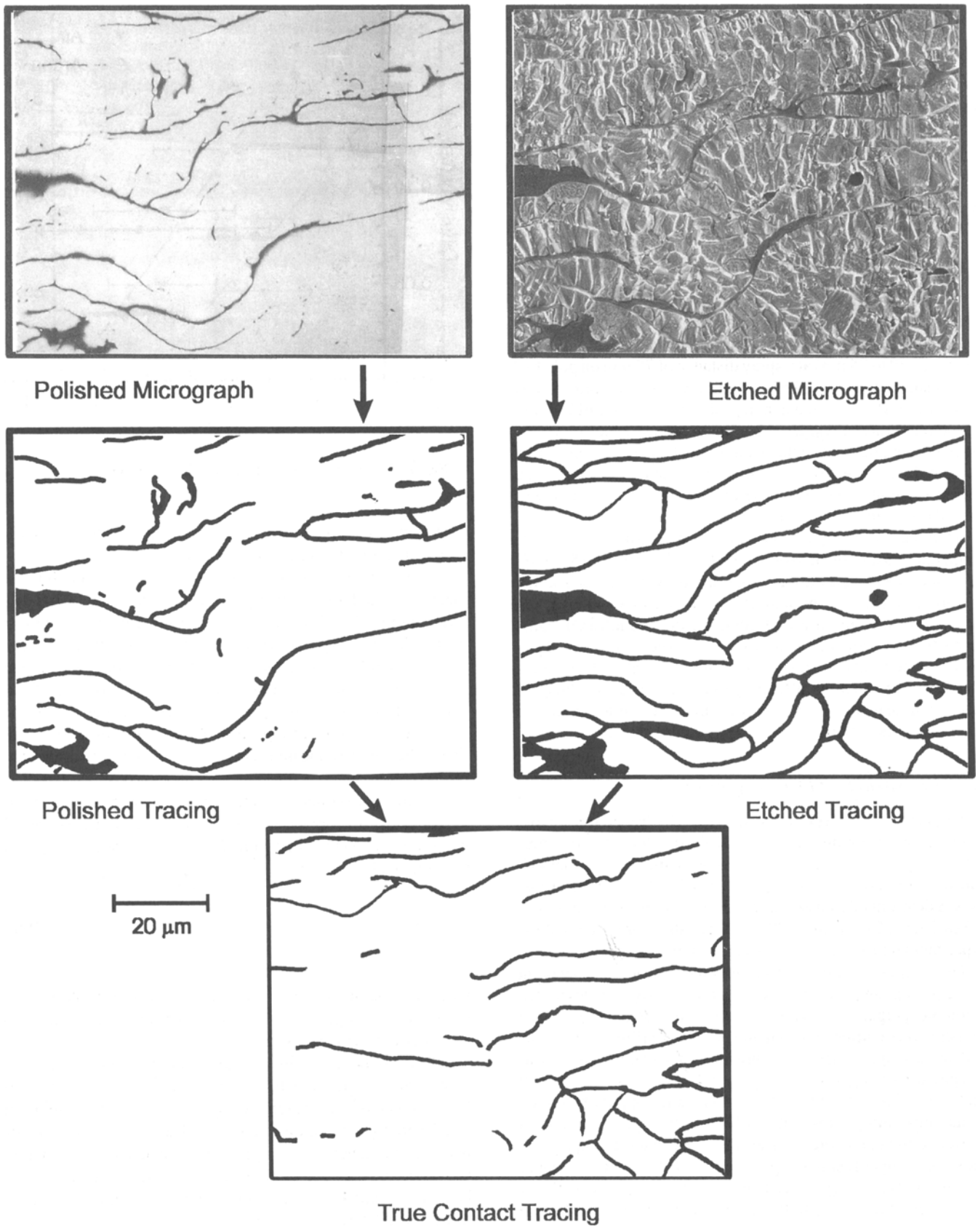

Fig. 2 Schematic procedure to obtain microstructural parameters, bonding rate, and true contact radius

$$\frac{1}{\alpha_c} = \frac{\rho_c C_{Pc}}{\lambda_c} = \frac{(1-F)}{\alpha_W}\left(1+\frac{1}{2nr\delta}\right) + \frac{(1-F)C_{Pw}\rho_W}{\lambda_o}\frac{\delta_o}{\pi nr^2\delta} \quad \text{(Eq 7)}$$

Note that the coating porosity influences the thermal diffusivity in two ways. The interlamellar porosity affects the lamellar resistance R_i, and the overall porosity affects the density of the coating.

3. Experimental Method

3.1 *Spray Conditions and Thermal Diffusivity Measurements*

Samples were sprayed using an SG100 Plasmadyne torch (129-145-130) with Metco 61 tungsten powder (purity 99.5%, size range 30 to 75 μm) at a spray distance of 75 mm on polished copper substrates (15 by 15 by 1.6 mm) cooled by a nitrogen jet at 40 L/min. Prior to tungsten deposition, a boron nitride spray was applied on the copper substrate to reduce adhesion of the tungsten coatings and detach them easily from the substrate without damage. A few coatings were sprayed on grit-blasted copper substrates. The spraying in controlled atmosphere was carried out in an airtight chamber.

Thermal diffusivity measurements were carried out at room temperature using the laser flash method (Ref 9). A 0.5 J YAG laser pulse (750 μs duration, 6 mm diam) was used to heat the coating surface, and the temperature of the rear surface was monitored using an infrared InSb detector. The infrared signal intensity was digitized using a 12-bit Nicolet 440 scope. Heat losses due to radiation and convection were negligible. Overestimation of the coating diffusivity due to the effect of three-dimensional heat propagation was estimated to be less than 6% and was neglected (Ref 6).

3.2 *Microstructural Investigation*

Oxygen contents were determined by a hydrogen weight loss technique based on the ASTM E 159-86 standard. The determination of specific surface was carried out using the BET method, with a gas mixture of 0.1% Kr and 99.9% He. The coating porosity was determined by a gravimetric method based on the ASTM B 328-73, C 357-85, and C20-83 standards. More details of the experimental procedure and results are given in Ref 7.

Direct microscopic observation of the samples is a key point of the present analysis. In order to avoid damage during metallographic preparation, samples were infiltrated with molten copper before cutting and polishing. Copper infiltration was carried out in a high-temperature furnace under a pure hydrogen atmosphere. Coatings on which a copper foil was placed were first heated at 1000 °C to reduce the tungsten and copper oxides and to maximize tungsten wettability by molten copper. Infiltration of the coating open porosity was then performed at temperature above the copper fusion temperature (1100 °C) (Ref 7). Copper was selected for two main reasons: its wetting angle is relatively low on solid tungsten, and there is no reaction between the two metals. All pores of the coatings were infiltrated, indicating that nearly 100% of the porosity was connected. Copper infiltration eliminates pullout and provides excellent metallographic contrast between copper and tungsten, making possible a quantitative evaluation of interlamellar porosity.

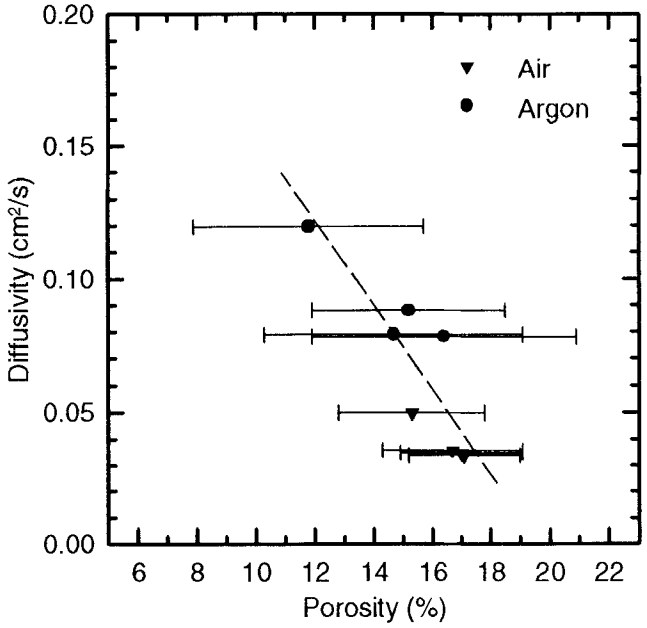

Fig. 3 Correlation between thermal diffusivity and porosity

The mean no contact quantity, mean true contact radius, and mean lamella thickness were measured with image analysis of micrographs of polished and etched cross sections. There were difficulties in using automatic image analysis software to identify the shape of the interfaces within the coating, so handmade tracing reproductions of these interfaces were made (Fig. 2). Images of these reproductions were grabbed and skeletonized before analysis, transforming the interfaces into one-pixel thick lines. The length of the interfaces was obtained from the number of line pixels.

The mean no contact quantity Q was obtained from the total length of the no contact regions in a cross-sectional surface. It was measured on the tracing images of the polished micrographs and is given by:

$$Q = \frac{n_i}{n_s \cdot l} \quad \text{(Eq 8)}$$

where l is the pixel width, n_i is the number of line pixels in the skeletonized image, and n_s is the number of line pixels in the total image area, respectively.

The mean bonding rate Φ is defined as the ratio of mean true contact area to the mean total interface area between the lamellae. In this case, measurements were carried out on both polished and etched sample images. Indeed, the number of line pixels of the etched images n_c is directly related to the total interface area, and the number of line pixels of the polished images n_i is directly related to the no contact area. The mean bonding rate Φ was then determined using:

$$\Phi = \left(1 - \frac{n_i}{n_c}\right) \quad \text{(Eq 9)}$$

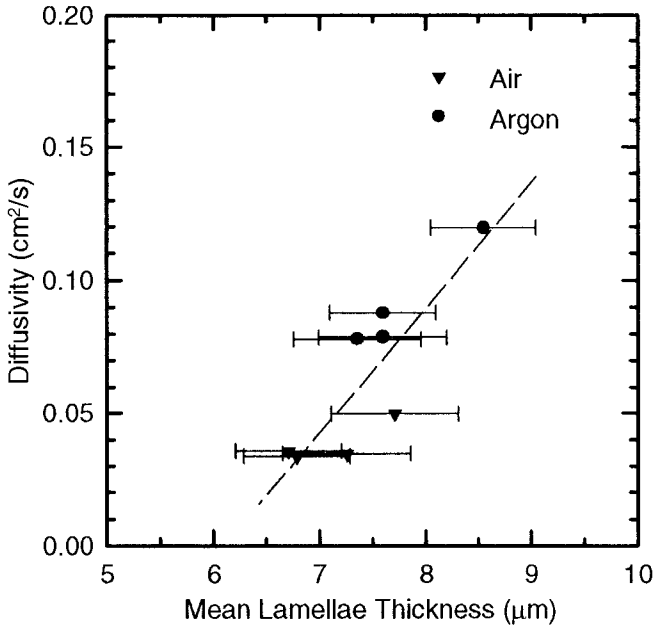

Fig. 4 Correlation between thermal diffusivity and mean lamellae thickness

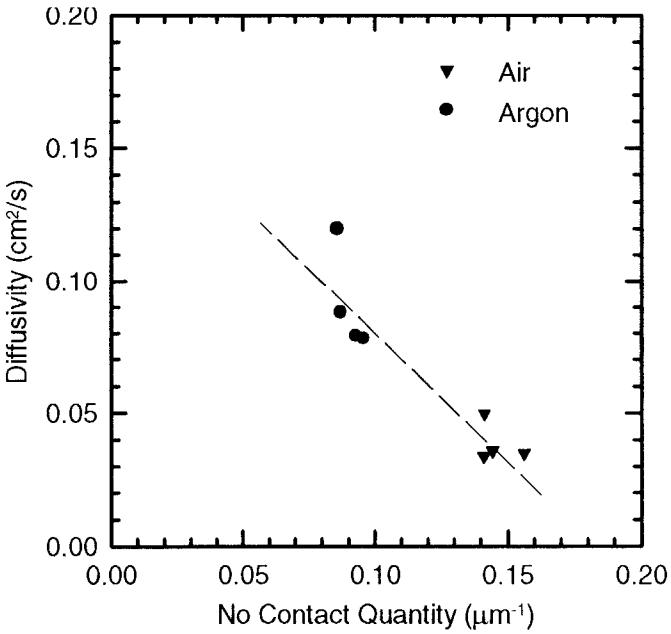

Fig. 6 Correlation between thermal diffusivity and no contact quantity

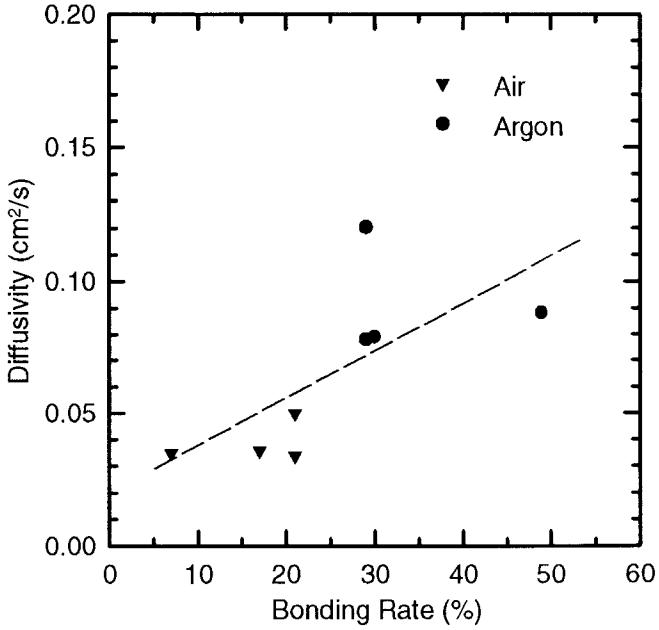

Fig. 5 Correlation between thermal diffusivity and bonding rate

As mentioned above, subtraction of the no contact area on polished tracing images from the total apparent interface on etched tracing images gives a new image, which represents the interlamellar true contact images. The mean radius of true contact regions r was measured on these resulting images:

$$r = \frac{4}{\pi m} \sum_{i=1}^{m} L_i \qquad \text{(Eq 10)}$$

where L_i is the intersection length of individual contact zones in the micrography plane and m is the number of individual contact zones taken to calculate the mean radius value r. The mean radius of true contact regions is related to the random intersection length of a circular zone by the factor $4/\pi$.

4. Results and Discussion

Figure 3 shows the correlation between thermal diffusivity and the coating porosity. Diffusivity decreases with increasing porosity. Coatings produced in argon have a lower porosity than those sprayed in air and have a higher thermal diffusivity.

As shown in Fig. 4, higher thermal diffusivity is reached when the lamellae are thicker. This is not surprising, because the number of thermal-resistant interfaces through the coating decreases with the lamella thickness.

The effect of the bonding rate on thermal diffusivity is shown in Fig. 5. Data are more scattered than those for other parameters. As expected, the thermal diffusivity increases with the mean bonding rate. It is worth noting that the spray atmosphere has a significant influence on the bonding rate. Indeed, it is lower than 20% in air-sprayed coatings and reaches 30 to 50% when spraying is performed in controlled atmosphere.

Figure 6 shows that thermal diffusivity decreases with the no contact quantity. It is important to clearly understand the difference between the bonding rate and the no contact quantity. The bonding rate represents the fraction of true contact at the interlamellar interfaces, while the no contact quantity represents the total area of no contact zones within the coating. The no contact quantity depends on both the bonding rate and the lamella thickness. Thermal diffusivity and conductivity depend on the bonding rate Φ at the lamella interfaces and on the number of these interfaces, and these properties are thus expected to depend strongly on the no contact quantity, as observed in Fig. 6. On the

other hand, the bonding rate should have a more direct influence on the mechanical cohesion of the coating.

4.1 *Estimation of the Coating Diffusivity*

In this section the thermal diffusivity of the coating is estimated by using the observed microstructural parameters and the model developed above. Table 1 gives the modeling parameters. Previous analyses have shown that the spraying atmosphere is the most influential spray factor on the coating thermal diffusivity (Ref 6), so one sample sprayed in air and one sprayed in argon with a similar porosity were chosen for this analysis (numbers 2 and 6 in Ref 7).

All parameters needed for calculations were determined experimentally except the oxide layer thickness, which was estimated from the specific surface and oxygen content values obtained previously (Ref 7). If one assumes that oxygen atoms are fixed in a thin oxide layer at the lamella surface, this layer thickness is estimated to be less than 70 nm in both the air- and argon-sprayed samples. The presence of oxygen at the surface of the lamellae in coatings produced in air was confirmed by Auger analysis. According to these analyses, the oxygen atomic concentration reached a maximum value of 25% at the lamella surface, indicating that the oxidized layer is composed of metallic tungsten and tungsten oxide. On the other hand, such an oxidized layer at the lamella surface was not detected in coatings sprayed in argon. Most of the oxide is thus likely to be distributed throughout the lamella thickness. It should be noted that the oxygen content in the coating sprayed in argon is significantly lower than that in the starting powders (0.19%).

Taking $\lambda_o = 26$ W/m·K at room temperature for tungsten oxide, the thermal resistance of the oxide layer R_o is thus about 24 times and 65 times lower than the interface resistance R_i in the samples sprayed in air and in argon, respectively. Consequently the oxide resistance can be neglected and Eq 7 reduces to:

$$\frac{1}{\alpha_c} = \frac{(1-F)}{\alpha_w}\left(1 + \frac{1}{2nr\delta}\right) \qquad \text{(Eq 11)}$$

Calculation of the resistances (Eq 2) and coating diffusivities (Eq 11) are summarized in Table 1.

The present results show that the difference of the thermal diffusivity observed in air- and argon-sprayed coatings cannot be attributed to oxide layer thermal resistance. Indeed, calculations show that the resistance of the oxide layer is small compared to the interlamellar interface resistance R_i. However, calculation of the thermal diffusivity shows a significant difference between air- and argon-sprayed coatings. This means that the thermal diffusivity of the coating is mainly ruled by the imperfect interlamellar contacts. Measured and calculated values are 0.034 and 0.020 cm^2/s, respectively, for the air-sprayed coating and 0.088 and 0.075 cm^2/s, respectively, for the argon-sprayed coating. It is important to note that the precision of the model is limited by the actual irregular lamellar structure of the coatings and the accuracy of microstructural parameters. Based only on these parameters, results indicate that argon-sprayed coatings should have a higher thermal diffusivity than coatings sprayed in air, as observed experimentally. Thus, lamella thickness, porosity, and interlamellar true contact radius have a great influence on coating diffusivity and seem to be sufficient to explain the difference in thermal diffusivity between air- and argon-sprayed tungsten samples.

Table 1 Microstructural parameters required for theoretical calculations of thermal diffusivity, with results

Microstructural parameter	Air-sprayed coating	Argon-sprayed coating
Specific surface, m^2/kg	64	46
Oxygen concentration, %	0.12	0.07
δ, μm	6.75	7.35
r, μm	5.73	9.16
n, $10^8 \times m^{-2}$	3.00	6.89
δ_o, nm	67	41
e, μm	490	515
F	0.167	0.164
R_r, m^2·K/W	2.0×10^{-6}	5.7×10^{-7}
R_o, m^2·K/W	8.3×10^{-8}	8.7×10^{-9}
α_{cal}, cm^2/s	0.020	0.075
α_{exp}, cm^2/s	0.034	0.088
α_w, cm^2/s	0.734	0.734

5. Conclusion

Copper-infiltrated tungsten coatings were successfully used to obtain, by direct microscopic observation, the mean bonding rate, the mean no contact quantity, and the mean true radius contact of the sprayed coatings. The mean no contact quantity is well correlated with the thermal diffusivity. Observations indicate that the oxide layer is very thin in coatings sprayed in air and practically absent in argon-sprayed coatings. Thus, calculations have shown that the effect of the oxide layer on thermal diffusivity is negligible and that the difference between air- and argon-sprayed coatings is essentially due to the interface imperfections. Spraying atmosphere has a strong influence on the contact quality and quantity between lamellae and thus on thermal diffusivity. This could be explained by many factors, such as temperature and gas heat transfer, but one particularly interesting factor is the presence of a thin oxide layer in air-sprayed coatings. It could drastically reduce the wetting of the impinging droplets on the already-solidified layers and thus reduce the bonding rate between lamellae, as established experimentally.

Acknowledgments

The authors wish to acknowledge Michel Thibodeau and Sylvain Bélanger for their technical assistance during the deposition and characterization of the sprayed coatings.

References

1. R.A. Neiser, G.R. Smolik, K.J. Hollis, and R.D. Watson, Evaluation of Plasma-Sprayed Tungsten for Fusion Reactors, *J. Thermal Spray Technol.*, Vol 2 (No. 4), 1993, p 393-399
2. R.E. Nygren and M.F. Smith, Beryllium: An Alternative Material for Plasma-Facing Components, *Fusion Technol.*, Vol 19, 1991, p 2092-2097
3. A. Ohmori and C.J. Li, Quantitative Characterization of the Structure of Plasma-Sprayed Al_2O_3 Coating by Using Copper Electroplating, *Thin Solid Films*, Vol 201, 1991, p 241-252
4. A. Ohmori, C.J. Li, and Y. Arata, The Structure of Plasma-Sprayed Alumina Coatings Revealed by Copper Electroplating, *Thermal Spray*

Coatings: Properties, Processes and Applications, T.F. Bernecki, Ed., ASM International, 1992, p 105-113

5. R. McPherson and B.V. Shafer, Interlamellar Contact within Plasma-Sprayed Coatings, *Thin Solid Films*, Vol 97, 1982, p 201-204
6. C. Moreau, P. Fargier-Richard, R.G. Saint-Jacques, and P. Cielo, Thermal Diffusivity of Plasma-Sprayed Tungsten Coatings, *Surf. Coat. Technol.*, Vol 61, 1993, p 67-71
7. S. Boire-Lavigne, C. Moreau, and R.G. Saint-Jacques, Taguchi Analysis of the Influence of Plasma Spray Parameters on the Microstructure of Tungsten Coatings, *Developments and Applications of Ceramics and New Metal Alloys*, R.A.L. Drew and H. Mostaghaci, Ed., Proc. International Symposium on Developments and Applications of New Ceramics and Metals Alloys, 1993, p 473-485
8. R. McPherson, A Model for the Thermal Conductivity of Plasma-Sprayed Coatings, *Thin Solid Films*, Vol 112, 1994, p 89-95
9. W.J. Parker, R.J. Jenkins, C.P. Butler, and G.L. Abbott, Flash Method of Determining Thermal Diffusivity, Heat Capacity, and Thermal Conductivity, *J. Appl. Phys*, Vol 32 (No. 9), 1961, p 1679-1684